UC Davis
UC Davis Previously Published Works

Title

Polyamines and eIF5A hypusination facilitate SREBP2 synthesis and cholesterol production leading to enhanced enterovirus attachment and infection

Permalink

Journal

ISSN

Authors

Firpo, Mason R
LoMascolo, Natalie J
Petit, Marine J
et al.

Publication Date

2023

DOI

Peer reviewed

Polyamines and eIF5A hypusination facilitate SREBP2 synthesis and cholesterol production leading to enhanced enterovirus attachment and infection

Mason R. Firpo[1], Natalie J. LoMascolo[1,2], Marine J. Petit[3,4¤], Priya S. Shah[3,4], Bryan C. Mounce[1,2]*

1 Department of Microbiology and Immunology, Stritch School of Medicine, Loyola University Chicago, Maywood, Illinois, United States of America, **2** Infectious Disease and Immunology Research Institute, Stritch School of Medicine, Loyola University Chicago, Maywood, Illinois, United States of America, **3** Department of Microbiology and Molecular Genetics, University of California, Davis, Davis, California, United States of America, **4** Department of Chemical Engineering, University of California, Davis, Davis, California, United States of America

¤ Current address: University of Glasgow MRC-Center for virus research, Glasgow, United Kingdom
* bmounce@luc.edu

Abstract

Metabolism is key to cellular processes that underlie the ability of a virus to productively infect. Polyamines are small metabolites vital for many host cell processes including proliferation, transcription, and translation. Polyamine depletion also inhibits virus infection via diverse mechanisms, including inhibiting polymerase activity and viral translation. We showed that Coxsackievirus B3 (CVB3) attachment requires polyamines; however, the mechanism was unknown. Here, we report polyamines' involvement in translation, through a process called hypusination, promotes expression of cholesterol synthesis genes by supporting SREBP2 synthesis, the master transcriptional regulator of cholesterol synthesis genes. Measuring bulk transcription, we find polyamines support expression of cholesterol synthesis genes, regulated by SREBP2. Thus, polyamine depletion inhibits CVB3 by depleting cellular cholesterol. Exogenous cholesterol rescues CVB3 attachment, and mutant CVB3 resistant to polyamine depletion exhibits resistance to cholesterol perturbation. This study provides a novel link between polyamine and cholesterol homeostasis, a mechanism through which polyamines impact CVB3 infection.

Author summary

Viruses rely on cellular metabolism for productive infection. How viruses interact with and manipulate metabolism impacts viral replication and pathogenesis. Metabolic pathways are frequently interconnected, and perturbation of one pathway can have wide-ranging impacts on other metabolites within the cell. Here, we show that polyamines, small positively-charged metabolites critical to virus infection, regulate cholesterol synthesis,

which ultimately impacts viral attachment. We find that polyamines' role in translation is
critical to their regulation of cholesterol synthesis. These data have important implications
for the connections between polyamine and sterol synthesis as well as how these molecules
impact virus replication.

Introduction

Polyamines are small carbon chains with amine groups that have a positive charge at cellular
pH. They play important roles within the cell and are involved in multiple cellular processes
including nucleotide synthesis, DNA/RNA stability, membrane fluidity, and translation [1].
Ornithine, which is a derivative of arginine, is converted to the first polyamine putrescine by
the rate limiting enzyme ornithine decarboxylase 1 (ODC1). Putrescine can be converted to
spermidine and spermine via their respective synthases. Difluoromethylornithine (DFMO), an
FDA-approved drug for trypanosomiasis, is an irreversible, competitive inhibitor of ODC1
[2]. One crucial way polyamines impact cells is through translation, specifically through a pro-
cess called hypusination [3]. Spermidine is covalently attached to eukaryotic initiation factor
5A (eIF5A) at lysine 50 by the protein deoxyhypusine synthase (DHPS) to form deoxyhypu-
sine-eIF5A. Deoxyhypusine hydroxylase (DOHH) then adds a hydroxyl group in the second
and final step to generate hypusine-eIF5A. eIF5A is the only known protein to be hypusinated
in eukaryotic cells. Hypusine-eIF5A plays a vital role in mRNA translation, ribosome function,
and cell proliferation [4,5]. The precise mechanisms by which hypusine-eIF5A promotes
translation remain to be fully understood; however, certain amino acid motifs cause ribosomal
pausing, and hypusine-eIF5A is required for the ribosome to translate through these motifs
[6]. Poly-proline tracts have also been shown to require hypusine-eIF5A [7]. When the unhy-
pusinated form of eIF5A is present, it cannot alleviate ribosomal pausing. The requirement for
hypusine-eIF5A for cellular proliferation has made it an attractive target for the development
of anti-cancer drugs. One such drug is the spermidine analog N1-guanyl-1,7-diaminoheptane
(GC7). GC7 inhibits DHPS by directly binding to the active site and prevents spermidine from
being attached to eIF5A [8]. Additionally, deferiprone (DEF) is an iron-chelator which has
broad effects on the cell and also inhibits DOHH [4].

Polyamines have been found to be important for RNA virus replication through different
mechanisms, and diverse RNA viruses are sensitive to DFMO-mediated polyamine depletion
[9–12]. Interestingly, the enterovirus Coxsackievirus B3 (CVB3) develops mutations within its
proteases as well as the capsid protein VP3 when polyamine synthesis is inhibited, suggesting a
role for polyamines in protease activity and cellular attachment of enteroviruses [13–15].
Enteroviruses are small, non-enveloped, positive sense single-stranded RNA viruses a part of
the picornavirus family that can cause a range of diseases from the mild cold to flaccid paralysis
and dilated cardiomyopathy (DCM) [16,17]. CVB3 is a member of the enterovirus genus and
is well known for its ability to infect and persist in the heart and cause DCM [18,19]. About
50% of DCM patients have CVB3 reactive antibodies, and the only cure for DCM is a heart
transplant [17,20]. There are currently no FDA drugs approved to treat CVB3 infection. How-
ever, we previously found that inhibiting polyamines inhibits CVB3 infection and binding
[13,14,21].

Another key metabolite required for CVB3 infection is cholesterol. Cholesterol is important
for maintaining cellular membrane integrity and fluidity as well as lipid raft formation.
Removal of cholesterol from the plasma membrane blocks poliovirus entry and EV-11 entry
by preventing lipid raft formation [22,23]. Inhibiting cholesterol homeostasis significantly

inhibits CVB3 replication [24]. The first step in cholesterol synthesis is the conversion of Ace-tyl-CoA to HMG-CoA by HMG-CoA synthase (HMGCS). HMG-CoA is then converted to mevalonic acid by the rate limiting enzyme HMG-CoA reductase (HMGCR). Cholesterol is produced after 27 more reactions. The majority of these synthetic genes are under the tran-scriptional control of sterol regulatory element binding protein 2 (SREBP2), which binds to sterol regulatory elements (SREs) in the promoter of target genes [25]. Upon depletion of cho-lesterol, the ER resident, multipass transmembrane protein, SREBP2 is translocated to the Golgi. Within the Golgi, it is cleaved by the proteases S1P and S2P generating the active N-ter-minal portion of the protein. The active SREBP2 then re-locates to the nucleus where it pro-motes the transcription of sterol synthesis genes [26]. To date, no link has been established between cholesterol synthesis and polyamines; however, mice overexpressing the polyamine catabolic enzyme spermidine-spermine acetyltransferase (SAT1) and rats treated with DFMO exhibited lower serum cholesterol levels [27,28], suggesting that polyamines may facilitate cho-lesterol synthesis.

Using a transcriptomic approach, we identified several pathways modulated by polyamines that likely impact enterovirus infection. We found that cholesterol synthesis genes were enriched in this analysis and hypothesized that polyamines may impact cholesterol synthesis and virus attachment. Here we describe a novel link between polyamines and cholesterol syn-thesis through the polyamine-dependent translation of SREBP2. We find that inhibition of polyamine synthesis or specific inhibition of hypusination leads to reduced SREBP2 synthesis, activity, and downstream gene expression. This culminates in reduced cellular cholesterol and, in turn, reduced viral attachment and replication. These data connect previously unrelated metabolic pathways in the cell and identify cellular cholesterol depletion as an important effect of polyamines on virus replication, with implications for both virus infection and cellular met-abolic status.

Results

Inhibition of polyamine synthesis inhibits CVB3 binding and is rescued with exogenous polyamines

We previously found that inhibition of polyamine synthesis by the specific inhibitor DFMO significantly decreases CVB3 binding to cells compared to untreated cells [14]. To confirm this phenotype, we treated Vero cells with increasing doses of DFMO to deplete cellular poly-amines. We then added CVB3 directly to cells on ice for 5 minutes. Virus was then washed off followed by agar overlay, in media containing polyamines. Thus, in these assays, polyamines are depleted only for attachment. CVB3 readily forms plaques on Vero cells and the Coxsack-ievirus and Adenovirus receptor (CAR) binding domain has 100% sequence identity com-pared to human CAR. Plaques generated from successful attachment and entry were allowed to form and developed two days later, and bound virus was enumerated by counting these pla-ques (Fig 1A). We found that DFMO significantly reduced bound virus in a dose-dependent manner (Fig 1B, above), in agreement with prior work and corresponding to a decrease in cel-lular polyamines, as measured by thin layer chromatography (Fig 1B, below). To determine if this polyamine-dependent attachment phenotype relied on cellular factors, we treated cells with DFMO to deplete polyamines and subsequently replenished the polyamines (putrescine, spermidine, and spermine) in an equimolar concentration. Adding polyamines to the cells at the time of infection did not rescue viral attachment, nor did addition 4h prior to attachment (Fig 1C). However, when polyamines were added 24h prior to infection, we observed a full res-cue in CVB3 attachment. These data suggest that polyamines rescue viral attachment but rely
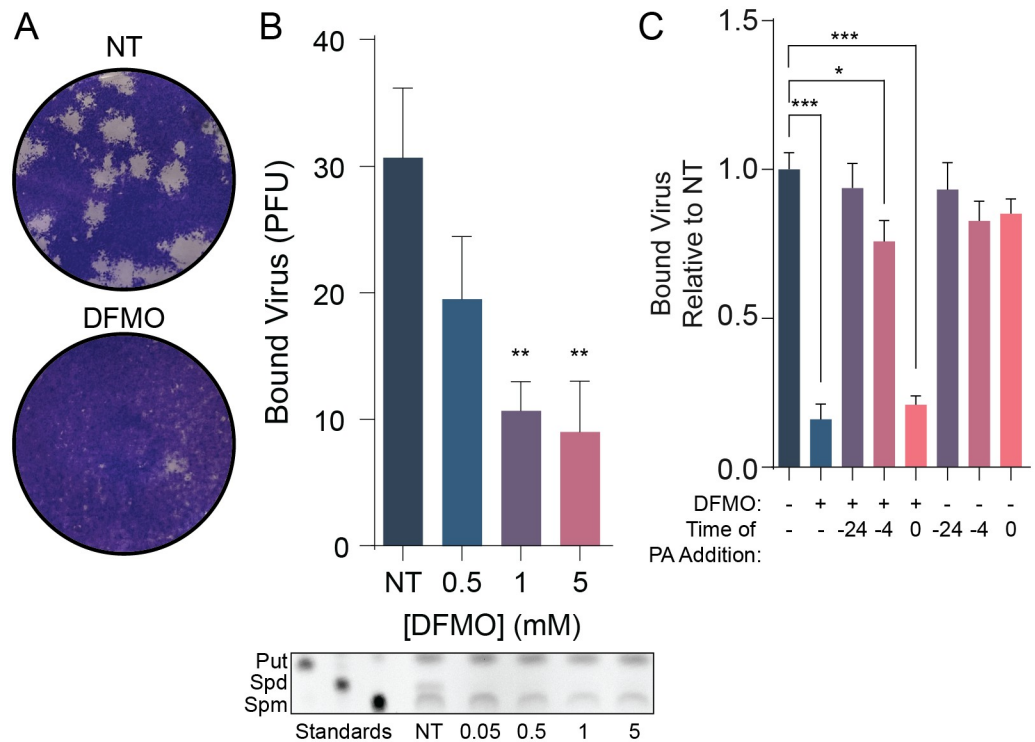
Fig 1. CVB3 requires polyamines for attachment. (A) Representative plaques from B. (B) (Top) Quantification of plaques formed from a CVB3 binding assay with DFMO treated Vero cells. (Bottom) Thin layer chromatography of Huh7 cells treated with increasing doses of DFMO. (C) Vero cells were treated with DFMO for 96 hours then treated with 10 μM equimolar ratio of polyamines at the indicated times before infection. $^*p < 0.05$, $^{**}p < 0.01$, $^{***}p < 0.001$ by the Student's t test. Data from at least three independent experiments. Error bars represent standard error.

on an extended incubation period, perhaps because cellular synthesis of attachment factors required this longer incubation time.

Polyamine depletion decreases expression of genes in the cholesterol synthesis pathway

To better understand the effects of polyamine depletion on cells and to identify polyamine-modulated cellular factors involved in viral attachment, we performed RNA-sequencing on untreated and polyamine-depleted cells. Huh7 cells were left untreated or depleted of polyamines with DFMO, at which time RNA was extracted and analyzed by Illumina paired-end reading. After the alignment of reads against the human genome, differential gene expression analysis was conducted to identify significant changes in expression. To uncover the underlying biological processes that may link these pathways, gene set enrichment analysis (GSEA) was performed. This showed multiple metabolic pathways that were significantly enriched for decreased gene expression by polyamine depletion including alcohol metabolism, cholesterol metabolism, and cellular response to a chemical (Fig 2A). In order to investigate specific cholesterol genes affected by DFMO, cholesterol genes involved directly in cholesterol synthesis were overlaid on a volcano plot (Fig 2B). Multiple genes were down regulated including HMGCS1, HMGCR, MVK, and MVD. Importantly, several polyamine metabolic genes, including SAT1 and OAZ1, exhibited reduced expression, consistent with their role in inhibiting polyamine synthesis. We next explored how these changes caused by DFMO related to changes caused by CVB3 infection. Again, differential gene expression analysis was performed
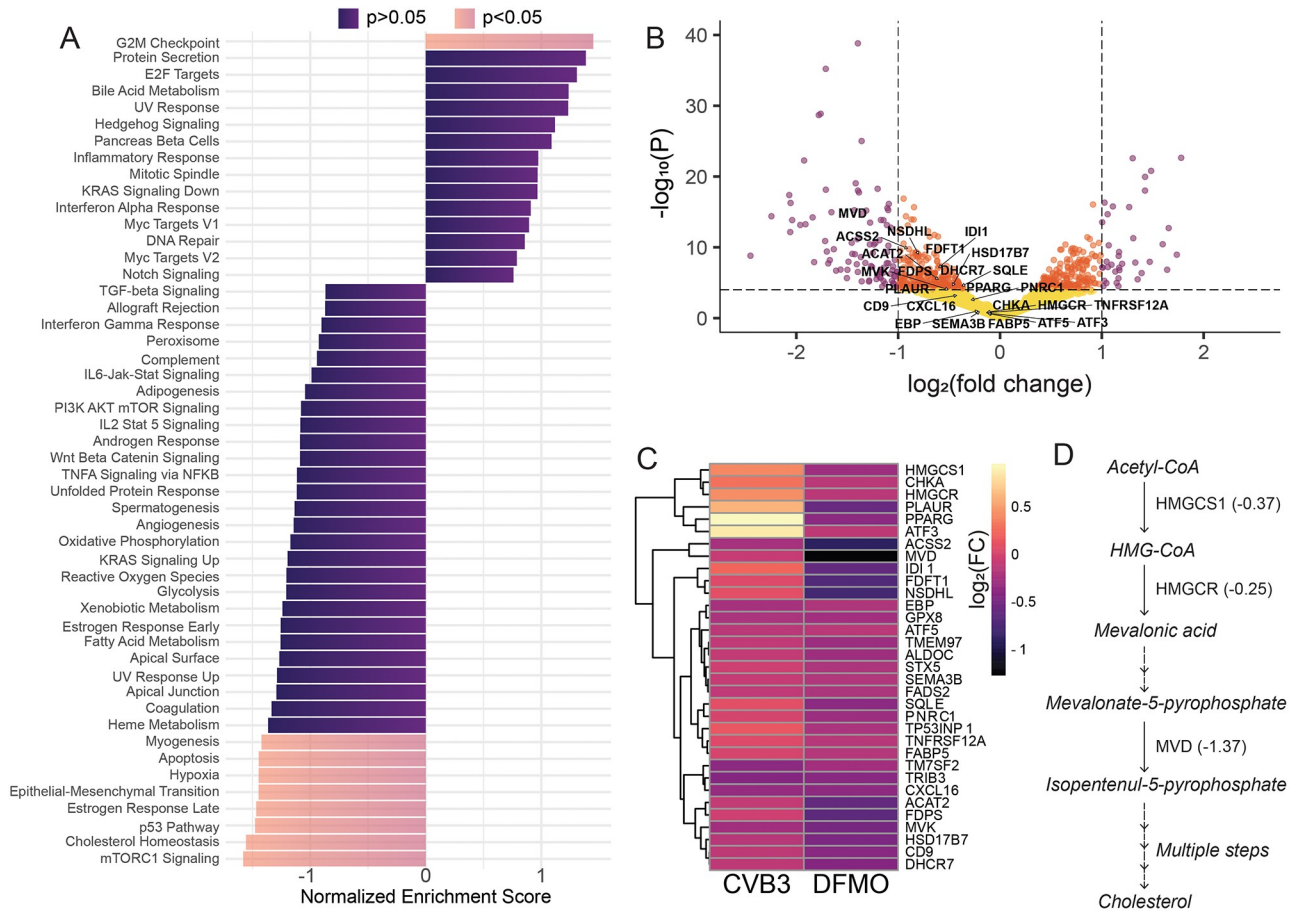
Fig 2. Transcriptomic analysis of DFMO treated cells. Huh7 cells were treated with 1mM DFMO for 96h and subjected to RNA sequencing. Results are based on duplicates. (A) GSEA was conducted on genes differentially expressed by 1mM DFMO treated Huh7 versus untreated Huh7. The top positively and negatively enriched Hallmark pathways were plotted (p.adj<0.05, purple, p.adj >0.05, blue). (B) Volcano plot indicating $\log_2$FoldChange for genes from differential gene expression analysis comparing DFMO treated cells relative to untreated cells. Significant changes in gene expression are plotted in purple for genes: p.adj<0.05, -1>$\log_2$FC>1, in orange for p.adj<0.05, -1<$\log_2$FC<1 and in yellow for p.adj>0.05, -1<$\log_2$FC<1. P-values were adjusted for false discovery rate using Benjamini Hochberg method. (C) Genes from the leading edge of cholesterol homeostasis pathway were subjected to hierarchical clustering for both conditions DFMO treated or CVB3 infected cells relative to untreated cells. $\log_2$ fold change from target genes are displayed as a heat map. (D) Cholesterol synthesis pathway with the representation of down-regulated genes HMGCS1, HMGCR and MVD. Values indicate fold change in gene expression.

https://doi.org/10.1371/journal.ppat.1011317.g002

on CVB3-infected and mock-treated cells. Leading edge genes from the "Cholesterol Homeostasis" category were visualized by heat map for CVB3-infected and DFMO-treated samples (Fig 2C). Interestingly, CVB3 infection increased expression of many cholesterol biosynthesis genes that are downregulated by DFMO, suggesting CVB3 has mechanisms to promote this pro-viral pathway. Thus, the transcriptomic analysis of polyamine depleted and virus-infected cells revealed that cellular metabolic processes and, specifically, cholesterol biosynthesis (Fig 2D) may function in a pro-viral manner.

Polyamine depletion decreases cholesterol gene expression, protein levels, and intracellular cholesterol

To test polyamines' effect on the transcription of cholesterol synthesis genes and confirm the RNA-seq data, cells were treated with increasing concentrations of DFMO. RNA was then

extracted and RT-qPCR was performed using optimized and specific primers. HMGCR, HMGCS, and MVD showed moderate but significant reductions in expression (Fig 3A-C), aligning with the RNA-sequencing data. To determine if this reduction in transcription affected protein synthesis, we examined total cellular levels of HMGCR and MVD by western blot. Both proteins showed reduced levels with polyamine depletion (Fig 3D). Finally, to determine if reduction of transcription and translation of cholesterol synthesis proteins affected intracellular cholesterol, cells were treated with DFMO, and total cellular cholesterol was measured via a luciferase-based cholesterol assay. We found that total cellular cholesterol was significantly reduced with DFMO treatment, consistent with a decrease in expression of cholesterol synthesis genes (Fig 3E). Thus, cellular cholesterol synthesis relies on polyamines through the expression of cholesterol synthetic proteins.

Polyamine-dependent SREBP2 translation but not transcription facilitates transcriptional activity at cholesterol gene promoters

Having observed that an array of cholesterol synthetic enzymes were reduced in transcription and translation by polyamine depletion, we considered that polyamines may affect a master regulator of their expression, rather than on each gene individually. We hypothesized that polyamines were affecting the transcription factor sterol regulatory binding protein 2 (SREBP2), one such regulator. SREBP2 is a multipass transmembrane protein found within the ER. When cholesterol levels are low within the cell, SREBP2 relocates to the Golgi where it is cleaved by S1P and S2P. The N-terminus of SREBP2 then relocates to the nucleus where it binds to sterol regulatory elements (SRE) to increase transcription of cholesterol synthesis genes. To test the impact polyamines have on SREBP2, Huh7 cells were treated with increasing doses of DFMO followed by qPCR (Fig 4A). Unlike the cholesterol synthetic genes, we observed no significant change in SREBP2 transcripts. However, examining SREBP2 protein levels by western blot revealed that polyamine depletion caused a reduction of SREBP2 protein (Fig 4B), though this reduction appeared to level off despite increasing doses of DFMO. To determine if this reduction of SREBP2 translation was sufficient to impact the expression of cholesterol synthesis genes, we measured the activity of SREBP2 binding to its promoter, the SRE. We transfected cells with or without polyamines with a construct encoding firefly luciferase driven by distinct cellular SREs (Fig 4C). We used the HMGCS SRE, the LDLR SRE, and a generalized SRE created with the SRE consensus sequence. Additionally, we transfected renilla luciferase to control for effects of polyamine depletion on luciferase translation. When we measured SRE activity, we noted a significant reduction in activity in polyamine depleted cells for all SREs tested, suggesting that polyamine depletion impacts SRE promoter activity, likely due to a reduction in SREBP2 synthesis. Thus, polyamines facilitate translation and activity but not transcription of SREBP2.

Polyamine-dependent eIF5A hypusination supports SREBP2 synthesis and cholesterol synthesis

A well-described mechanism by which polyamines support cellular translation is through the post-translational modification of eIF5A, in which spermidine is conjugated and hydroxylated, forming a unique amino acid called hypusine (summarized in Fig 5A). eIF5A is currently the only known protein to undergo hypusination in eukaryotic cells. Hypusinated eIF5A facilitates translation on a subset of cellular proteins often containing polyproline tracts [7]. We first confirmed that DFMO treatment reduced levels of hypusinated eIF5A (Fig 5B). To determine if SREBP2 is included in the subset of cellular proteins sensitive to hypusination, we treated cells the deoxyhypusine synthase (DHPS) inhibitor GC7. GC7 treatment reduced SREBP2 protein
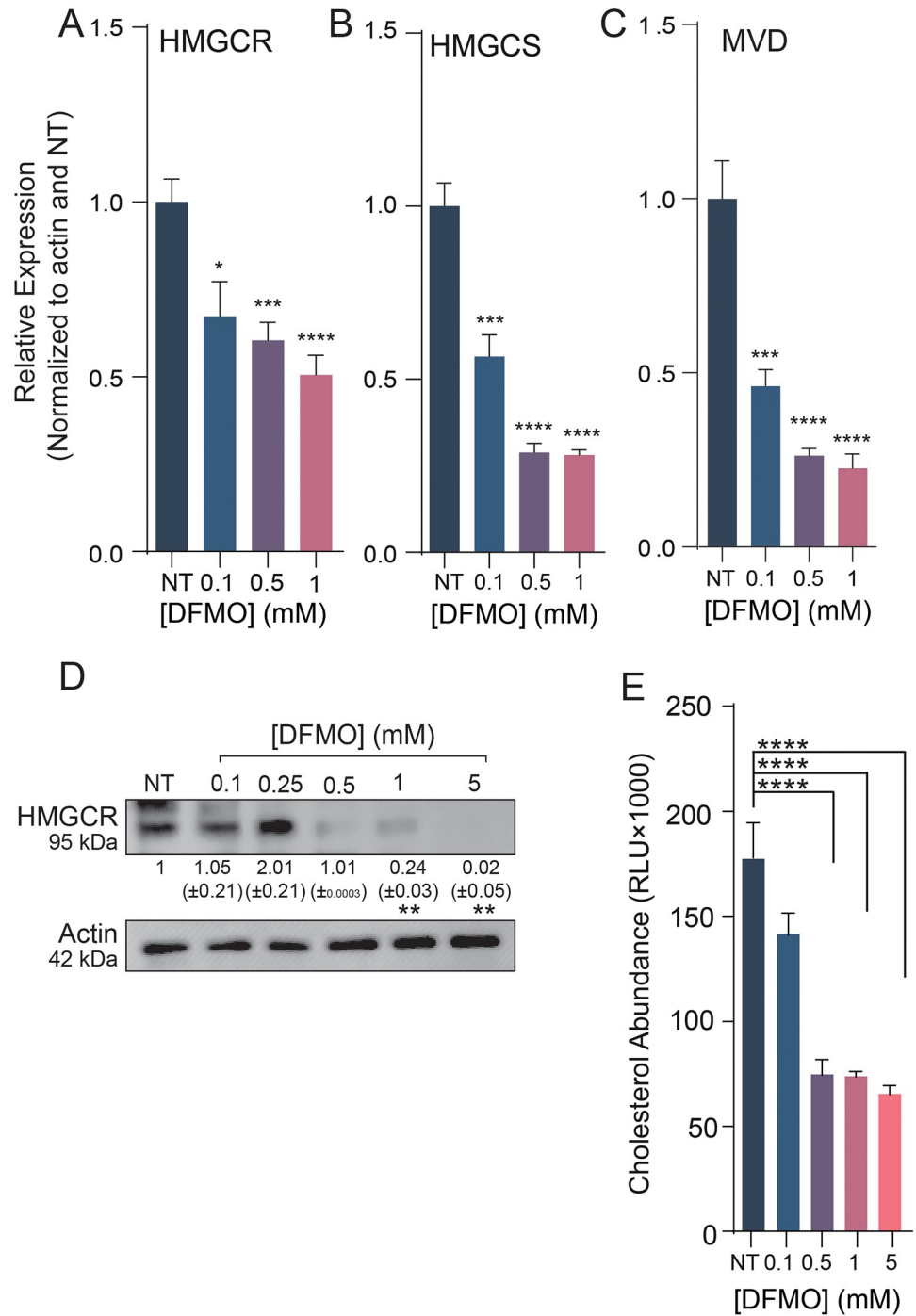
Fig 3. Depletion of polyamines decreases cholesterol synthesis gene expression, translation, and intracellular abundance. (A-C) Normalized qPCR of cholesterol synthesis genes relative to actin expression in Huh7 cells treated with DFMO for 96h. (D) Western blot of Huh7 cells treated with increasing doses of DFMO. Actin was used as a loading control. (E) Intracellular cholesterol abundance in DFMO treated Huh7 cells. $*p < 0.05$, $**p < 0.01$, $***p < 0.001$, and $****p < 0.0001$ by the Student's t test. Data from at least three independent experiments. Error bars represent standard error.
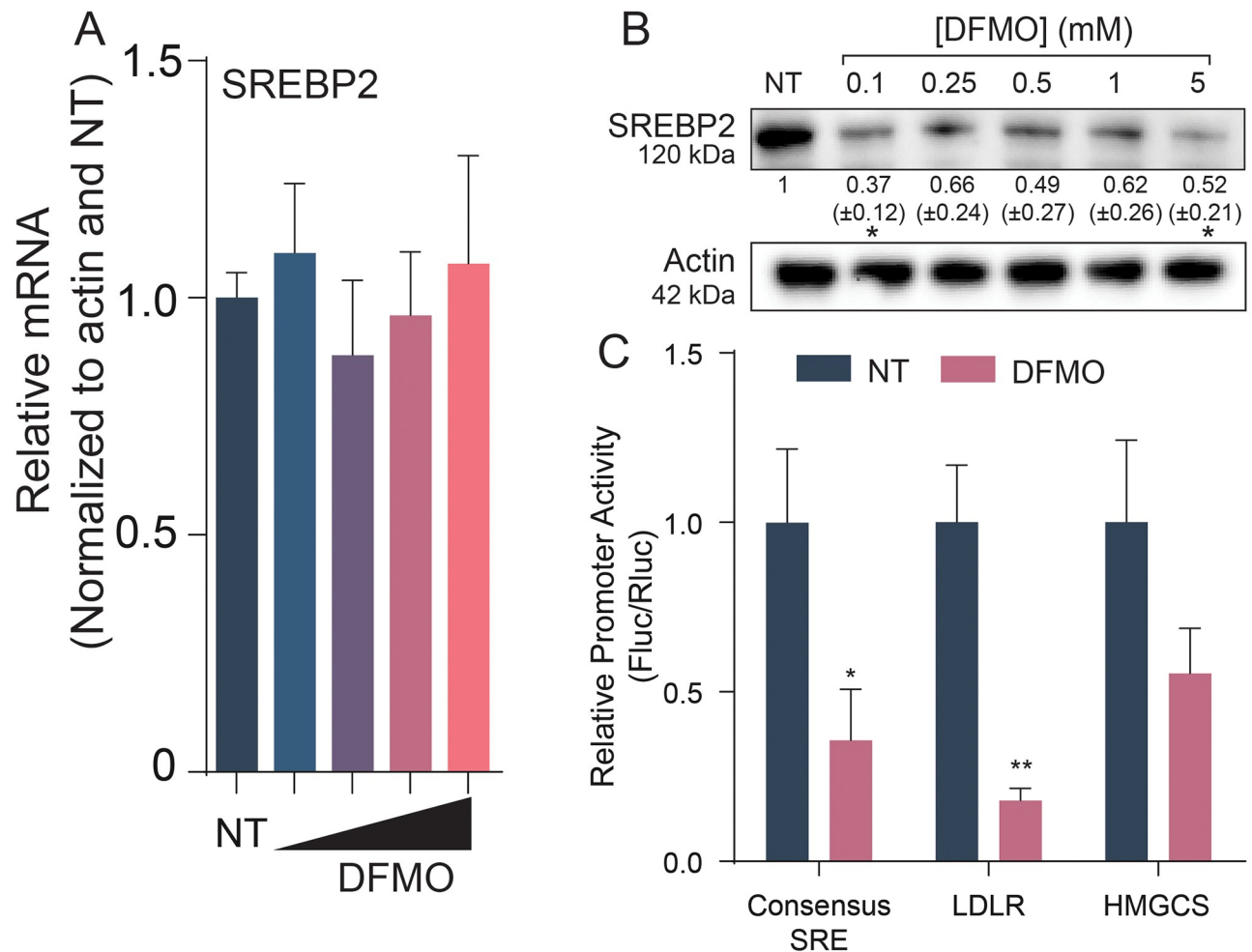
Fig 4. SREBP2 synthesis is dependent on polyamines. (A) Normalized qPCR of SREBP2 with increasing doses of DFMO (0.1, 0.5, 1, 5mM) relative to actin expression in Huh7 cells. (B) Western blot of SREBP2 in DFMO treated Huh7 cells. Actin was used as a loading control. (C) Huh7 cells were treated with 1mM DFMO for 96h followed by transfection with the promoter luciferase constructs and renilla luciferase transfection controls. Results are normalized to no treatment (NT) and are relative to renilla activity. $^*p < 0.05$ and $^{**}p < 0.01$ by two-way ANOVA. Data from at least three independent experiments.

levels in a dose-dependent manner, concomitant with a reduction in cellular hypusinated eIF5A (Fig 5C), though no change in total eIF5A levels was observed. SREBP2 mRNA expression with GC7 treatment resulted in no significant changes in gene expression (Fig 5D) as seen with DFMO and consistent with a role for hypusination in translation. Further, we observed no significant change in viability with GC7 treatment (Fig 5E). In concurrence with this, treatment with GC7 resulted in significant reduction of SRE promoter activity (Fig 5F). Additionally, we observed a reduction in HMGCR protein levels with increasing GC7 or deferiprone (DEF) treatment (Fig 5G). To confirm that these changes in SREBP2 and cholesterol synthesis gene expression affected cellular cholesterol, we measured total cellular cholesterol in cells treated with increasing doses of GC7 (Fig 5H). Similar to our results with DFMO, we observed a significant, dose-dependent reduction in cellular cholesterol when hypusination was inhibited, suggesting that polyamines facilitate cholesterol synthesis through hypusination. We further confirmed this phenotype with DEF treatment, which also resulted in reduced total cellular cholesterol (Fig 5I). SREBP2 contains di-proline motifs within its N-terminal domain,
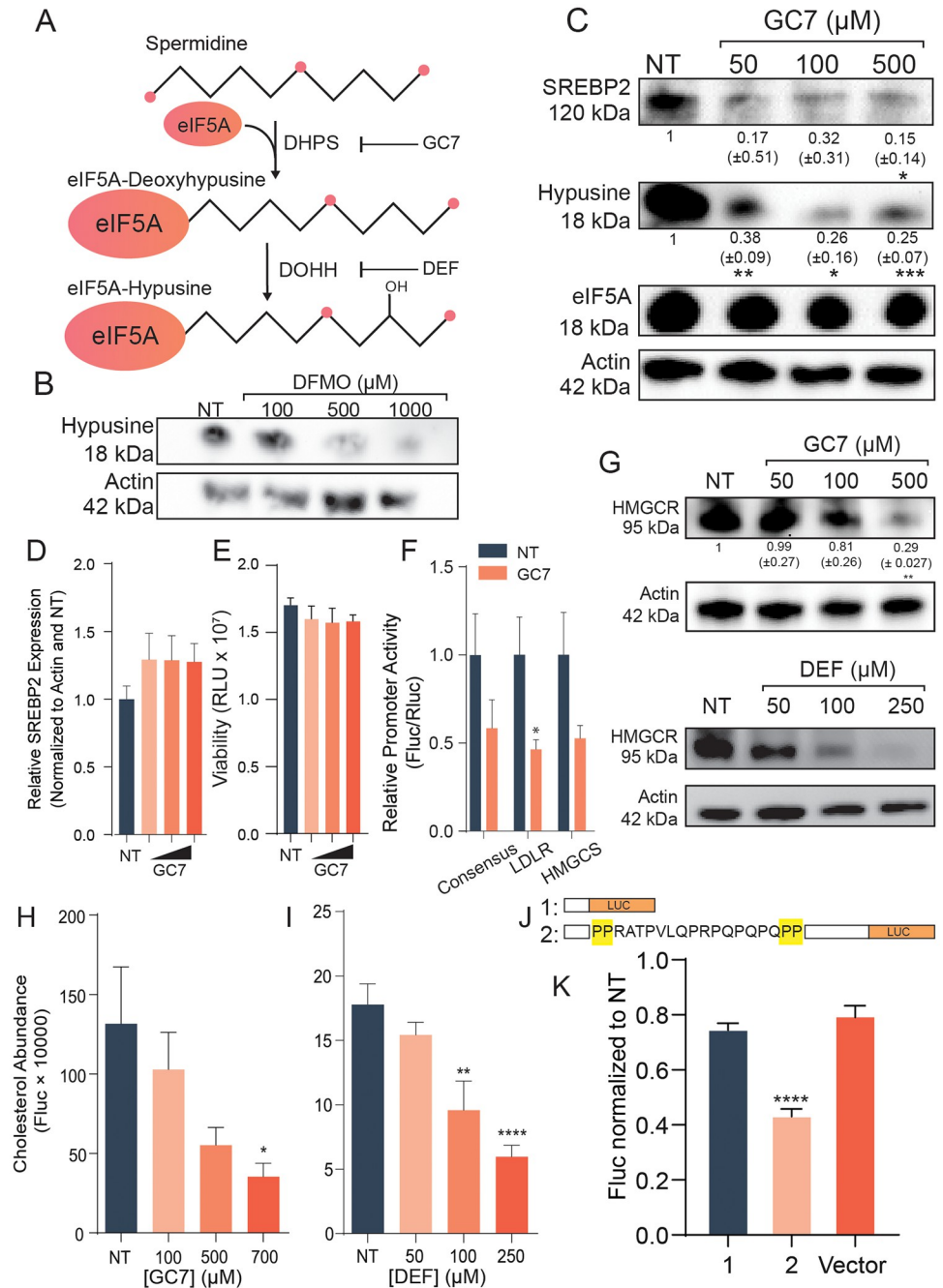
Fig 5. Hypusination supports cholesterol synthesis. (A) Pathway of eIF5A hypusination and its inhibition. (B) Huh7 cells were treated with increasing doses of DFMO and analyzed by western blot for hypusinated eIF5A. (C) Western blot of Huh7 cells treated with increasing doses of GC7 probed for SREBP2, hypusine-eIF5A, and total eIF5A. (D) Huh7 cells were treated with increasing doses of GC7 and SREBP2 transcription measured by qRT-PCR. (E) Cells were treated as in (D) and analyzed for viability after 24h of treatment. (F) Huh7 cells treated with 500 μM GC7 for 24h followed by transfection with the SRE promoter luciferase constructs and renilla luciferase as a transfection control. Results were normalized to untreated conditions, relative to renilla luciferase activity. Two-way ANOVA was used to analyze statistical significance. (G) Western blot of Huh7 cells treated with increasing doses of GC7 or deferiprone (DEF) and probed for HMGCR. (H, I) Intracellular cholesterol abundance of GC7- and DEF-treated Huh7 cells. (J) Constructs of SREBP2 fused to luciferase used in (K) to measure translation after GC7 treatment. Firefly luciferase activity was measured and normalized to renilla luciferase activity, comparing untreated to GC7 treatment conditions. $^*p < 0.05$, $^{**}p < 0.01$, $^{***}p < 0.001$, and $^{****}p < 0.0001$ by the Student's t test. Data from at least three independent experiments.

https://doi.org/10.1371/journal.ppat.1011317.g005

which are a known motif sensitive to eIF5A hypusination [7]. To determine if these di-prolines are responsible for the decrease in SREBP2, we designed SREBP2 fragments, stopping before (construct 1) or containing diproline motifs (construct 2), in pLenti-CMV-Luc (summarized in Fig 5J). We transfected these constructs into cells treated with 500 µM GC7 and measured luminescence 24h later and normalized to untreated cells (Fig 5K). We observed a significant reduction in luminescence for the polyproline-containing fragment (construct 2) compared to construct 1, lacking the diproline motif. There was no significant difference in luminescence between fragment 1 and the vector, suggesting that the reduction in translation with fragment 2 was specific to the sequence containing the diproline motif.

Exogenous cholesterol rescues CVB3 attachment to polyamine depleted cells and replication

Viruses require diverse cellular factors to mediate attachment and entry, including cholesterol. To determine if cholesterol is a key polyamine-modulated molecule in this process, we attempted to rescue viral attachment and replication by adding cholesterol to cells exogenously. Cells depleted of polyamines were treated with increasing doses of cholesterol overnight, followed by washing away excess cholesterol and performing a binding assay as before. When plaques were revealed, we found that cholesterol significantly rescued CVB3 binding in a dose dependent manner (Fig 6A). To determine if adding in cholesterol was able to rescue the amount of bound genomes, we performed a binding assay as described above, but collected bound virus in Trizol and analyzed via qPCR (Fig 6B). Polyamine depletion significantly decreased the amount of bound genomes while the addition of cholesterol was able to significantly rescue bound genome to polyamine depleted cells. We confirmed that adding exogenous cholesterol restored cholesterol to basal conditions (Fig 6C). To test if this rescue was due to a direct interaction of CVB3 and cholesterol or if cholesterol had to be incorporated into cellular membranes, cholesterol was added to cells at 22h, 4h, and 0h before CVB3 binding. Only cholesterol added 22h and 4h before binding was able to significantly rescue CVB3 binding to polyamine depleted cells (Fig 6D), suggesting that viral attachment requires cellular cholesterol incorporation. We next considered the cholesterol transport inhibitor U18666A, which works by inhibiting NPC-1, critical for cholesterol transport within the cell [29]. U18666A treatment of cells significantly reduced bound CVB3 (Fig 6E), confirming a role for cholesterol in CVB3 attachment. Finally, to determine if cholesterol could rescue virus replication in polyamine-depleted cells, we measured viral titers in DFMO- and cholesterol-treated cells. DFMO significantly reduced viral titers, and treatment with exogenous cholesterol significantly increased these titers, though not to untreated levels, highlighting that polyamines affect cholesterol to support viral replication but also that polyamines play multiple roles in infection (Fig 6F). To confirm that hypusinated eIF5A contributes to viral attachment, as we see with DFMO, we treated cells with increasing doses of GC7, performed an attachment assay, and counted attached viruses (Fig 6G). We observed a dose-dependent decrease of viral attachment with GC7 treatment, suggesting hypusinated eIF5A facilitates viral attachment. Inhibiting hypusination also significantly reduced the amount of bound genomes (Fig 6H). We are also able to partially rescue viral attachment to GC7 treated cells with cholesterol (Fig 6I). Again, we confirmed that adding exogenous cholesterol restored cellular cholesterol to basal levels with GC7 treatment (Fig 6J).

We previously described a viral mutant that exhibits enhanced viral attachment in polyamine depleted cells via mutation of VP3 at position 234 (VP3^{Q234R}) [14]. This mutant was found when we passaged virus in DFMO-treated cells, suggesting that CVB3 harboring this mutation may be resistant to polyamine depletion by overcoming a block in attachment. To
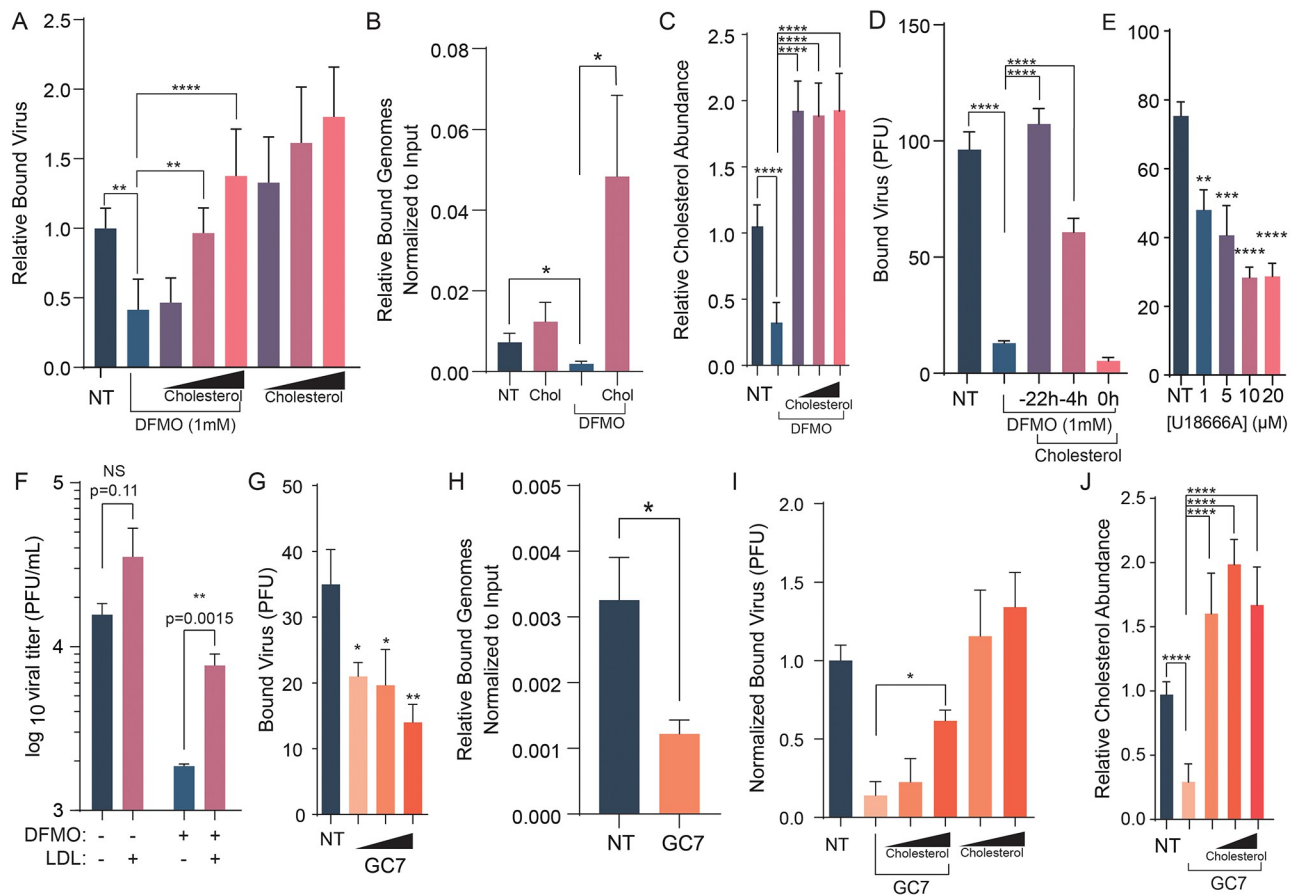
Fig 6. Addition of cholesterol rescues CVB3 attachment and replication in polyamine depleted cells. (A) Binding assay of Vero cells, left untreated or treated with DFMO for 96h. After 72h, cells were treated with 100, 250, or 500 μg/mL cholesterol for 24h prior to performing the binding assay. (B) Vero cells were treated with 1mM DFMO for 96h. After 72h, cells were treated with 250 μg/mL cholesterol for 24h prior to performing qPCR attachment assay. (C) Total cellular cholesterol was measured in cells treated with DFMO and supplemented with increasing doses of exogenous cholesterol. (D) Binding assay of DFMO-treated Vero cells treated with 500 μg/mL cholesterol at the indicated times. (E) Binding assay of Vero cells treated with increasing concentrations of U1866A, a cholesterol transport inhibitor. (F) Huh7 cells were left untreated or treated with DFMO for 96h. After 72h, the cells were treated with 100 μg/mL LDL for 24h followed by infection with CVB3 at an MOI of 0.1. Virus was collected after 24h and the titer determined by plaque assay. (G) Vero cells were treated with increasing doses of GC7 and viral attachment measured via binding assay. (H) Vero cells were treated with 250 μM GC7 for 24h and viral attachment was measured via qPCR. (I) Vero cells treated with GC7 were supplemented with exogenous cholesterol and viral attachment measured by binding assay. (J) Cells treated as in (G) were assayed for total cellular cholesterol levels. $^*p < 0.05$, $^{**}p < 0.01$, $^{***}p < 0.001$, and $^{****}p < 0.0001$ by the Student's t test. Data from at least three independent experiments.

https://doi.org/10.1371/journal.ppat.1011317.g006

determine if this block was cholesterol-dependent, we considered viral attachment in cells where cholesterol transport is impaired. We found that treatment of cells with U18666A reduced CVB3 attachment in a dose-dependent manner (Fig 7A), as well as replication (Fig 7B). We next considered that CVB3 VP3[Q234R] may be resistant to this inhibitor. When we performed an attachment assay on U18666A treated cells using CVB3 VP3[Q234R], we observed a modest reduction in viral attachment compared to WT CVB3, suggesting that the mutant may overcome polyamine depletion via bypassing the need for cholesterol (Fig 7A). Additionally, we measured viral titers in U18666A-treated cells infected with CVB3 VP3[Q234R] and observed titers significantly higher than WT CVB3 (Fig 7B). Together, these data suggest that polyamines support cholesterol synthesis to promote viral attachment and that CVB3 is able to overcome polyamine depletion by mutation of VP3, which bypasses the need for cholesterol in viral attachment.
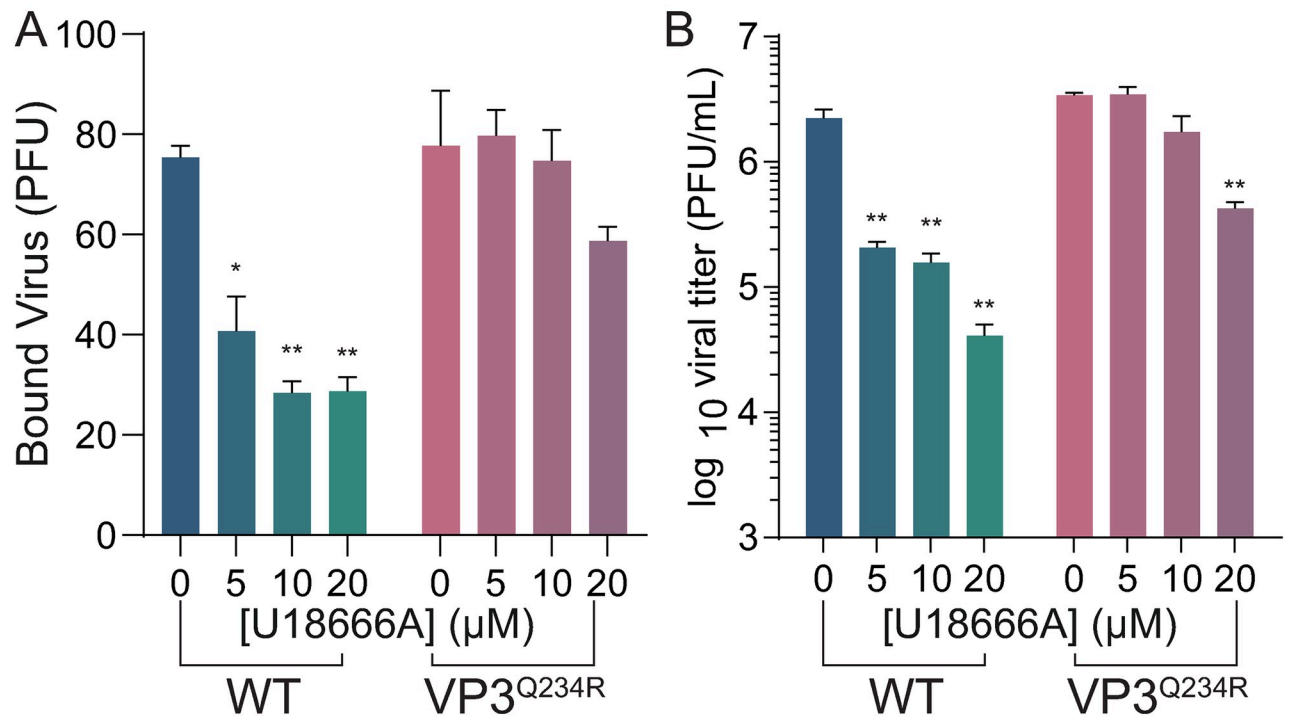
Fig 7. CVB3 VP3^{Q234R} mutant is resistant to reduction of cytoplasmic cholesterol. (A) Vero cells were treated with increasing doses of U18666A for 16h prior to binding WT and VP3^{Q234R} mutant CVB3. Bound virus was enumerated by counting plaques indicative of attached virus. (B) Vero cells were treated as in (A) and infected at MOI 0.1 with WT and VP3^{Q234R} mutant CVB3. Viral titers were determined at 24 hpi. *$p<0.05$, **$p<0.01$ via Student's t test from three independent experiments.

https://doi.org/10.1371/journal.ppat.1011317.g007

Discussion

Polyamines function in diverse ways within the cell [30–32], and their connections to distinct metabolic pathways are still being discovered. Here, we establish a novel connection between polyamines and cholesterol synthesis. Prior work has described how animal models treated with DFMO exhibited altered serum lipid profiles, though the molecular mechanisms remained unexplored [27,28]. We found that polyamines support intracellular cholesterol levels through the hypusination of eIF5A, which is required for translation of SREBP2, a key regulator in cholesterol homeostasis. This results in reduced SREBP2 protein levels when cells are treated with DFMO or when hypusination is specifically inhibited. The reduction of SREBP2 causes a significant reduction of sterol synthesis gene expression, culminating in reduced cellular cholesterol. This polyamine-mediated cholesterol depletion also effects CVB3's ability to attach to cells, and this binding is rescued when cholesterol is added to cells (Fig 8).

The process of hypusination has been well studied and defined [4,5,33]. Hypusine-eIF5A is required for cellular proliferation and translation of "hard-to-read" sequences, such as poly-proline motifs [7,34]. However, the specific genes that require hypusine-eIF5A for their translation are not well known. Here we have found that SREBP2 requires hypusine-eIF5A to be translated. While HMGCR does not have any poly-prolines, it does have a 3 amino acid motif, GGT, at position 807, that has been shown to be require hypusine-eIF5A [6]. SREBP2 on the other hand, has multiple poly-proline repeats as well as other 3 amino acid motifs shown to require hypusine-eIF5A. Furthermore, a study found hypusine-eIF5A is involved in cotranslation translocation of proteins into the ER, where SREBP2 is found [35]. Our findings demonstrate another level of regulation of the cholesterol synthesis pathway, translational regulation
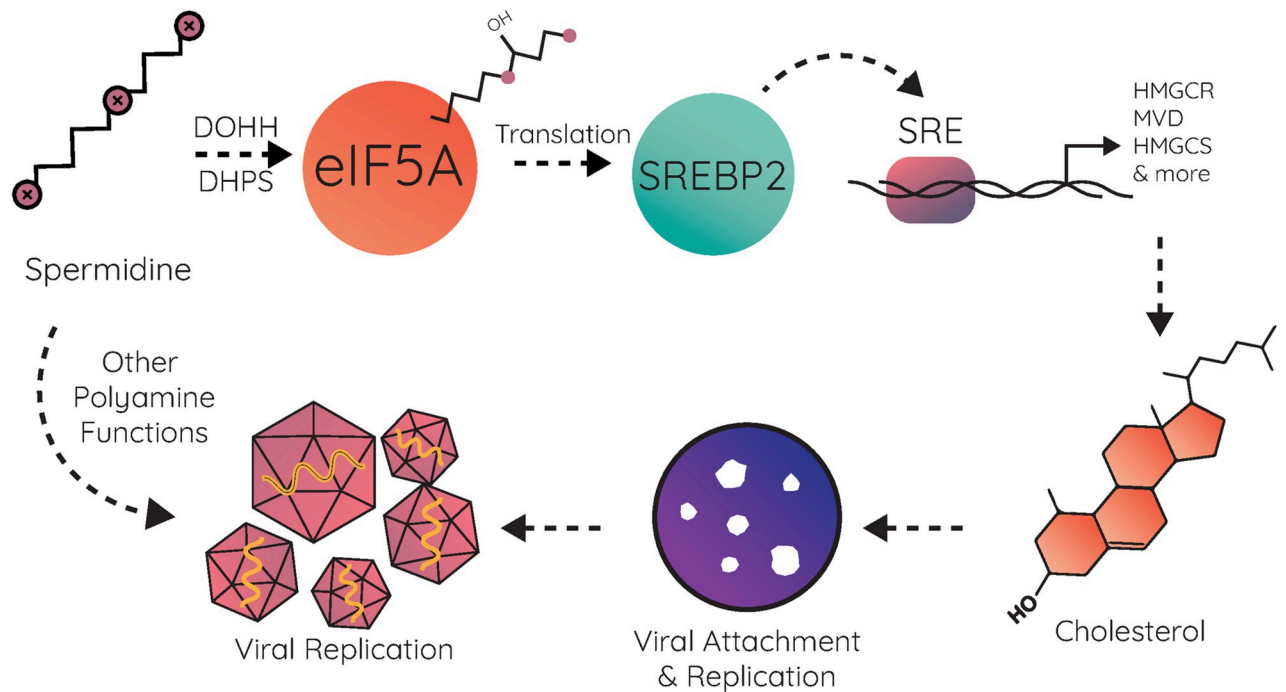
Fig 8. Working model. Polyamines facilitate hypusination of eIF5A, which promotes SREBP2 synthesis. SREBP2 binds to SREs on the promoters of cholesterol synthesis genes, leading to their expression and cholesterol synthesis. Cellular cholesterol synthesis enhances CVB3 attachment and, subsequently viral replication.

https://doi.org/10.1371/journal.ppat.1011317.g008

of SREBP2. Polyamines are vital for cellular proliferation, and a lack of polyamines will prevent crucial proliferation genes from being translated, such as SREBP2.

The roles of polyamines in viral infection are diverse and appear to be distinct for different viral families [1,30]. In the case of enteroviruses, like CVB3, prior work showed that polyamines facilitate cellular attachment and protease activity. However, the mechanism(s) by which polyamines promote these activities was unclear. Importantly, we observed that cellular attachment to DFMO-treated cells was reduced for a variety of viruses, including distinct picornaviruses (rhinovirus, enterovirus) [14]. Thus, it is unlikely that a reduction in receptor expression is sufficient to explain this broad phenotype. Cholesterol is a key molecule in enterovirus attachment and entry, and its association with lipid rafts has been demonstrated to facilitate CVB3 engagement with its receptor (Coxsackie- and adenovirus receptor, CAR) [36]. For many viruses, cholesterol and lipids promote not only entry, but also viral replication, either through the formation of viral replication compartments on specific cellular members or through the hydrolysis of lipids to release energy for replication [22,24,37–41]. While polyamines have previously been described to facilitate viral genome replication for both chikungunya virus [42] and Ebolavirus [10], it remains to be determined if this phenotype could be through the synthesis of cellular cholesterol. Prior work highlighted effects of polyamines on viral proteins, such as the polymerase [42], but our work highlights an indirect effect on virus infection, specifically through cholesterol synthesis. Further, this observation could explain the broad effect on viral attachment we observe with DFMO. Because polyamine depletion abrogates the attachment of diverse viruses, cellular cholesterol depletion in those cells may explain these phenotypes due to the key roles for cholesterol in virus attachment.

Although we show that SREBP2 relies on polyamines for translation through hypusinated eIF5A, regulation of SREBP2 and its activity is complex. Polyamines play a wide variety of

roles within the cell, one of which is stabilizing DNA and promoting transcription factor engagement [31]. Another potential area of involvement for polyamines within the cholesterol pathway is the stabilization of SREBP2 binding of SRE. It has previously been shown that polyamines maintain the estrogen receptor elements (ERE) in the correct motif to allow for estrogen receptor (ER) to bind, and a lack of polyamines decreased the ability of ER to bind to EREs [43,44]. Polyamines also play a role in protease function. Our lab previously demonstrated that both of CVB3's proteases develop mutations in response to polyamine depletion, making them resistant to the lack of polyamines, suggesting a role for polyamines in protease activity [13,15]. SREBP2 processing requires two proteases, S1P and S2P, for its maturation. It is unclear whether SREBP2 cleavage or S1P/S2P protease activity relies on polyamines. It is unlikely that hypusine-eIF5A is affecting another protein upstream of SREBP2 as its transcript levels do not significantly change with DFMO (Fig 4A) or GC7 (Fig 5D) treatment.

eIF5A is the only known enzyme within the eukaryotic cell to be hypusinated, and it supports the translation of diverse cellular proteins. Prior work showed that Ebolavirus relies on hypusination specifically for the translation of VP30, a viral transactivator that facilitates viral gene expression [45]. Other work showed that inhibitors of hypusination reduce translation of retroviruses, including HIV-1 [46,47]. The direct roles of eIF5A hypusination in viral protein synthesis remain to be fully explored for many viruses, including CVB3. However, hypusinated eIF5A's roles in cellular translation also affect viral replication, as seen here. Thus, hypusinated eIF5A is an important drug target due to its potential direct and indirect effects on virus replication [48]. Additional exploration of mechanisms connecting hypusinated eIF5A to viral and cellular factors involved in infection will further illuminate how this molecule and polyamines support the replication of diverse viruses.

Materials and methods

Cell culture and virus enumeration

Cells were maintained in Dulbecco's modified Eagle's medium (DMEM; Life Technologies) with bovine serum (FBS; Thermo-Fischer) and penicillin-streptomycin at 37˚C and 5% CO_2. Huh7 cells were supplemented with 10% fetal bovine serum (FBS; Thermo-Fischer). Vero cells were obtained through BEI Resources. Vero cells were supplemented with 10% new-born calf serum (NCBS; Thermo-Fischer). CVB3 (Nancy strain) was derived from the first passage of virus in Vero cells after rescue from an infectious clone. Viral stocks were maintained at -80˚C. Viral titers were enumerated as previously described [14].

Drug treatments

Difluoromethylornithine (DFMO; TargetMol) was diluted to a 100mM solution in sterile water. For DFMO treatments, cells were trypsinized and reseeded with fresh medium supplemented with 2% FBS (Huh7) or 2% NCBS (Vero). Cells were treated with 1mM DFMO unless otherwise indicated. Cells were incubated with DFMO for 96h to allow for depletion of polyamines. GC7 was diluted to a 100mM solution in sterile water. Freshly seeded cells were treated with GC7 along with 500μM aminoguanidine for 16-24h. Cholesterol was diluted to 10 $^{mg}/_{mL}$ in ethanol then added to adherent cells for 16-24h.

RNA purification and cDNA synthesis

Media were cleared from cells, and Trizol reagent (Zymo Research) was added directly. Lysate was then collected, and RNA was purified through a Zymo RNA extraction kit. Purified RNA was subsequently used for cDNA synthesis using High Capacity cDNA Reverse Transcription

Kits (Thermo-Fischer), according to the manufacturer's protocol, with 10–100 ng of RNA and random hexamer primers.

RNA sequencing

RNA was purified and prepared as described from Huh7 cells treated for 96h with DFMO or infected for 24h with CVB3. Libraries were prepared by the University of Chicago Genomics Facility and analyzed by Illumina NovaSeq 6000. Read quality was evaluated using FastQC (v0.11.5). Adapters were trimmed in parallel to a quality trimming (bbduk, sourceforge.net/projects/bbmap/). All remaining sequences were mapped against the human reference genome build 38 with STAR (v2.5.2b) [49]. HTseq (v0.6.1) was used to count all reads for each gene and set up a read count table [50]. Differential gene expression analyses were performed using the DESeq2 Bioconductor package (v1.30.1) [51]. The default "ashr" shrinkage (v2.2–47) [52] set up was used for our analysis. Gene set enrichment analysis (GSEA) was performed with the fgsea Bioconductor package [53], using Hallmark gene sets downloaded from the Molecular Signatures Database [54].

Plaque formation attachment assay

Vero cells were seeded in 6-well plates and grown to 100% confluence in DMEM with 2% NCBS and treated for 96h with the indicated concentrations of DFMO. After 96 h of DFMO treatment, cells were placed on ice and the media aspirated from the cells. 500 uL of serum free media containing 1000 PFU CVB3 was added to cells on ice for 5 min. Cells were washed 3x with PBS and then overlaid with 0.8% agarose containing DMEM with 2% NCBS. The plates were incubated at 37°C for 2 days for plaques to develop. The cells were fixed with 4% formalin, and the plaques were visualized with crystal violet staining. For the cholesterol rescue, cells were washed 3x with PBS before infecting with CVB3.

Cell viability

Huh7 cells were plated in a 96 well plate with 2% FBS DMEM, then treated for 24 hours with amino guanidine alone or in combination with increasing concentrations of GC7. After 24 hours, viability was measured using the CytoTox-Fluor Cytotoxicity Assay (Promega) according to the manufacturer's protocol.

qPCR Gene expression assay

Huh7 cells were seeded at 4×10^4 cells per well in 24-well plates in DMEM with 2% FBS. Cells were treated with varying concentrations of DFMO for 96 h. After 96 h, the media was aspirated off cells, washed 1x with PBS, and then, 200 uL of Trizol was added to the cells. The RNA was extracted with the Zymo RNA extraction kit, converted to cDNA, and quantified by real-time PCR with SYBR Green (DotScientific) using the one-step protocol QuantStudio 3 (ThermoFisher Scientific). Relative expression was calculated using the $\Delta\Delta C^T$ method, normalized to the β-actin qRT-PCR control, and calculated as the fraction of the untreated samples. Primers were verified for linearity using 8-fold serial diluted cDNA and checked for specificity via melt curve analysis. The primer sequences are as follows: HMGCR, (F) 5'-GAG ACA GGG ATA AAC CGA GAA AG-3' and (R): 5'-GGA GGA GTT ACC AAC CAC AAA-3'; HMGCS, (F): 5'-CCT GCC AAG AAA GTA CCA AGA-3' and (R): 5'-GTC TTG CAC CTC ACA GAG TAT C-3'; MVD (F): 5'-TGG TTC TGC CCA TCA ACT C-3' and (R): 5'-GGT GAA GTC CTT GCT GAT GA-3'; SREBP2 (F): 5'-CTG TAG CGT CTT GAT TCT CTC C-3' and (R): 5'-CCT GGC TGT CCT GTG TAA TAA-3'.

qPCR attachment assay

Vero cells were seeded at 4×10^4 per well in a 24 well plate with 2% NCBS DMEM respectively. Cells were treated with GC7 for 24h or with DFMO for 96h. Cholesterol was added to indicated samples for 24h. Cells were placed on ice, media removed, and CVB3 at MOI 5 in 100 uL SFM was then added directly to cells for 5 minutes. Input samples were then collected in TRIzol. Bound samples were washed 3x in PBS then collected in TRIzol. RNA was then extracted, purified, then reverse transcribed as described. cDNA was then quantified by real-time PCR with SYBR Green as described. Relative genomes were calculated using the $\Delta\Delta C^T$ method with actin and normalized to input virus.

Western blot

Samples were collected with Bolt LDS Buffer and Bolt Reducing Agent (Invitrogen, Waltham, MA, USA) and run on polyacrylamide gels. Gels were transferred using the iBlot 2 Gel Transfer Device (Invitrogen). Membranes were blocked with 5% BSA in TBST then probed with primary antibodies for HMGCR (Ms mAb, 1:000, Abcam), MVD (1:1000, Santa Cruz), SREBP2 (goat pAb, 1:1000, R&D Systems), Hypusine (Rb pAb, 1:2000, EMD Millipore) or β-actin (Ms mAb, 1:1000, Proteintech) overnight at 4˚C. Membranes were then washed 3x in TBST followed by 1h incubation of in secondary antibody (GtαMs/GtαRb/DonkeyαGt HRP, 1:15000, Jackson Labs). After 3 additional washes in TBST, membranes were treated with SuperSignal West Pico PLUS Chemiluminescent Substrate (ThermoFisher Scientific) and visualized on Fluorchem E imager (Protein Simple, San Jose, CA, USA). Quantification of western blots were done by using ImageJ and normalizing to NT and relative to actin density.

Intracellular cholesterol abundance assay

Huh7 cells were plated at a density of 5000 cells/well in a 96 well plate in DMEM with 2% FBS. Cells were treated with DFMO for 96h or after 72h, treated with DEF or GC7 for 24h. The following day, the media was removed from cells followed by a PBS wash. To measure total intracellular cholesterol abundance, we used the Cholesterol/Cholesterol Ester-Glo Assay (Promega) in accordance to manufacturer's protocol.

SRE promoter luciferase

Complimentary primers were made containing SRE consensus sequence were ordered flanked by SfiI cut site overhangs (FWD: 5'-CGGCC ATCACCCCAC GGCCTCGG-3'; REV 3'-GCCGCCGG TAGTGGGGTG CCGGA-5'). Primers were phosphorylated and annealed at 37˚C for 30 minutes then 95˚C for 5 minutes and were allowed to cool to 25˚C. pGL4.10 (Promega) was digested with SfiI in Fast Digest buffer for 15 min at 50˚C. The cut plasmid was ran through DNA clean up kit. The annealed primers were then ligated into the cut plasmid using T4 ligase followed by transformation into chemical competent E. Coli. Colonies were picked and grown up followed by sequencing to confirm the SRE sequence was present.

Promoter luciferase assay

Huh7 cells were plated in a 96 well plate with 2% FBS DMEM then treated with 1 mM DFMO for 96 h or after 96 h, treated with 500 μM GC7. Cells were transfected with SRE-pGL4.10, 5' HMGCS-Fluc (Addgene #60444), or pLDLR-Luc (Addgene #14940) after cells had been plated for 96 h. All cells were transfected with the renilla control plasmid (siCheck, Promega). 100 ng of plasmid were transfected with LipoD293 according to manufacture's protocol. 24h after

transfection, media was removed followed by one wash with PBS. Cells were then lysed with gentle lysis buffer for 15 min.

SREBP2 luciferase assay

SREBP2 fragment 1 contained nucleotides 3348–3798 and fragment 2 contained nucleotides 3348–4400 from Addgene #32018 (pLKO-puro FLAG SREBP2, murine SREBP2) were cloned into pLenti-CMV-Luc by Applied Biological Materials Inc. Huh7 cells were plated in a 96 well plate and treated with 500 μM for 24h. Cells were transfected with 100 ng of plasmid were transfected with LipoD293 according to manufacturer's protocol. 24h after transfection, media was removed followed by one wash with PBS. Cells were then lysed with gentle lysis buffer for 15 min.

Statistical analysis

Prism 6 (GraphPad) was used to generate graphs and perform statistical analysis. For all analyses, a two-tailed Student's *t* test was used to compare groups, unless otherwise noted.

Acknowledgments

Author Contributions

Conceptualization: Bryan C. Mounce.

Data curation: Mason R. Firpo, Bryan C. Mounce.

Formal analysis: Mason R. Firpo, Bryan C. Mounce.

Funding acquisition: Mason R. Firpo, Priya S. Shah, Bryan C. Mounce.

Investigation: Mason R. Firpo, Natalie J. LoMascolo, Marine J. Petit, Bryan C. Mounce.

Methodology: Mason R. Firpo, Natalie J. LoMascolo, Marine J. Petit, Priya S. Shah, Bryan C. Mounce.

Project administration: Bryan C. Mounce.

Resources: Bryan C. Mounce.

Software: Marine J. Petit, Priya S. Shah.

Supervision: Priya S. Shah, Bryan C. Mounce.

Validation: Mason R. Firpo, Natalie J. LoMascolo, Bryan C. Mounce.

Visualization: Mason R. Firpo, Marine J. Petit, Bryan C. Mounce.

Writing – original draft: Mason R. Firpo, Bryan C. Mounce.

Writing – review & editing: Mason R. Firpo, Natalie J. LoMascolo, Marine J. Petit, Priya S. Shah, Bryan C. Mounce.

References

1. Mounce BC, Olsen ME, Vignuzzi M, Connor JH. Polyamines and Their Role in Virus Infection. Microbiol Mol Biol Rev MMBR. 2017;81. https://doi.org/10.1128/MMBR.00029-17 PMID: 28904024

2. Burri C, Brun R. Eflornithine for the treatment of human African trypanosomiasis. Parasitol Res. 2003; 90 Supp 1: S49–52. https://doi.org/10.1007/s00436-002-0766-5 PMID: 12811548

3. Park MH, Cooper HL, Folk JE. Identification of hypusine, an unusual amino acid, in a protein from human lymphocytes and of spermidine as its biosynthetic precursor. Proc Natl Acad Sci U S A. 1981; 78: 2869–2873. https://doi.org/10.1073/pnas.78.5.2869 PMID: 6789324

4. Park MH, Joe YA, Kang KR, Lee YB, Wolff EC. The polyamine-derived amino acid hypusine: its post-translational formation in eIF-5A and its role in cell proliferation. Amino Acids. 1996; 10: 109–121. https://doi.org/10.1007/BF00806584 PMID: 24178473

5. Park MH, Wolff EC. Hypusine, a polyamine-derived amino acid critical for eukaryotic translation. J Biol Chem. 2018; 293: 18710–18718. https://doi.org/10.1074/jbc.TM118.003341 PMID: 30257869

6. Schuller AP, Wu CC-C, Dever TE, Buskirk AR, Green R. eIF5A Functions Globally in Translation Elongation and Termination. Mol Cell. 2017; 66: 194–205.e5. https://doi.org/10.1016/j.molcel.2017.03.003 PMID: 28392174

7. Gutierrez E, Shin B-S, Woolstenhulme CJ, Kim J-R, Saini P, Buskirk AR, et al. eIF5A Promotes Translation of Polyproline Motifs. Mol Cell. 2013; 51: 35–45. https://doi.org/10.1016/j.molcel.2013.04.021 PMID: 23727016

8. D'Agostino M, Motta S, Romagnoli A, Orlando P, Tiano L, La Teana A, et al. Insights Into the Binding Mechanism of GC7 to Deoxyhypusine Synthase in Sulfolobus solfataricus: A Thermophilic Model for the Design of New Hypusination Inhibitors. Front Chem. 2020; 8: 1170. https://doi.org/10.3389/fchem.2020.609942 PMID: 33392152

9. Mounce BC, Cesaro T, Vlajnić L, Vidiņa A, Vallet T, Weger-Lucarelli J, et al. Chikungunya Virus Overcomes Polyamine Depletion by Mutation of nsP1 and the Opal Stop Codon To Confer Enhanced Replication and Fitness. J Virol. 2017; 91. https://doi.org/10.1128/JVI.00344-17 PMID: 28539441

10. Olsen ME, Cressey TN, Mühlberger E, Connor JH. Differential Mechanisms for the Involvement of Polyamines and Hypusinated eIF5A in Ebola Virus Gene Expression. J Virol. 2018; 92. https://doi.org/10.1128/JVI.01260-18 PMID: 30045993

11. Mastrodomenico V, Esin JJ, Graham ML, Tate PM, Hawkins GM, Sandler ZJ, et al. Polyamine depletion inhibits bunyavirus infection via generation of noninfectious interfering virions. J Virol. 2019; JVI.00530-19. https://doi.org/10.1128/JVI.00530-19 PMID: 31043534

12. Firpo MR, Mastrodomenico V, Hawkins GM, Prot M, Levillayer L, Gallagher T, et al. Targeting Polyamines Inhibits Coronavirus Infection by Reducing Cellular Attachment and Entry. ACS Infect Dis. 2020; acsinfecdis.0c00491. https://doi.org/10.1021/acsinfecdis.0c00491 PMID: 32966040

13. Dial CN, Tate PM, Kicmal TM, Mounce BC. Coxsackievirus B3 Responds to Polyamine Depletion via Enhancement of 2A and 3C Protease Activity. Viruses. 2019; 11: 403. https://doi.org/10.3390/v11050403 PMID: 31052199

14. Kicmal TM, Tate PM, Dial CN, Esin JJ, Mounce BC. Polyamine depletion abrogates enterovirus cellular attachment. J Virol. 2019; JVI.01054-19. https://doi.org/10.1128/JVI.01054-19 PMID: 31341056

15. Hulsebosch BM, Mounce BC. Polyamine Analog Diethylnorspermidine Restricts Coxsackievirus B3 and Is Overcome by 2A Protease Mutation In Vitro. Viruses. 2021; 13: 310. https://doi.org/10.3390/v13020310 PMID: 33669273

16. Pons-Salort M, Parker EPK, Grassly NC. The epidemiology of non-polio enteroviruses: recent advances and outstanding questions. Curr Opin Infect Dis. 2015; 28: 479–487. https://doi.org/10.1097/QCO.0000000000000187 PMID: 26203854

17. Massilamany C, Gangaplara A, Reddy J. Intricacies of cardiac damage in coxsackievirus B3 infection: Implications for therapy. Int J Cardiol. 2014; 177: 330–339. https://doi.org/10.1016/j.ijcard.2014.09.136 PMID: 25449464

18. Chapman NM, Kim K-S. Persistent Coxsackievirus Infection: Enterovirus Persistence in Chronic Myocarditis and Dilated Cardiomyopathy. Group B Coxsackieviruses. Springer, Berlin, Heidelberg; 2008. pp. 275–292. PMID: 18357775

19. Garmaroudi FS, Marchant D, Hendry R, Luo H, Yang D, Ye X, et al. Coxsackievirus B3 replication and pathogenesis. Future Microbiol. 2015; 10: 629–653. https://doi.org/10.2217/fmb.15.5 PMID: 25865198

20. Archard LC, Bowles NE, Cunningham L, Freeke CA, Olsen EGJ, Rose ML, et al. Molecular probes for detection of persisting enterovirus infection of human heart and their prognostic value. Eur Heart J. 1991; 12: 56–59. https://doi.org/10.1093/eurheartj/12.suppl_d.56 PMID: 1655452

21. Mounce BC, Cesaro T, Moratorio G, Hooikaas PJ, Yakovleva A, Werneke SW, et al. Inhibition of Polyamine Biosynthesis Is a Broad-Spectrum Strategy against RNA Viruses. J Virol. 2016; 90: 9683–9692. https://doi.org/10.1128/JVI.01347-16 PMID: 27535047

22. Danthi P, Chow M. Cholesterol Removal by Methyl-β-Cyclodextrin Inhibits Poliovirus Entry. J Virol. 2004; 78: 33–41. https://doi.org/10.1128/JVI.78.1.33-41.2004

23. Stuart AD, Eustace HE, McKee TA, Brown TDK. A Novel Cell Entry Pathway for a DAF-Using Human Enterovirus Is Dependent on Lipid Rafts. J Virol. 2002; 76: 9307–9322. https://doi.org/10.1128/jvi.76.18.9307-9322.2002 PMID: 12186914

24. Ilnytska O, Santiana M, Hsu N-Y, Du W-L, Chen Y-H, Viktorova EG, et al. Enteroviruses harness the cellular endocytic machinery to remodel the host cell cholesterol landscape for effective viral replication. Cell Host Microbe. 2013; 14: 281–293. https://doi.org/10.1016/j.chom.2013.08.002 PMID: 24034614

25. Hua X, Yokoyama C, Wu J, Briggs MR, Brown MS, Goldstein JL, et al. SREBP-2, a second basic-helix-loop-helix-leucine zipper protein that stimulates transcription by binding to a sterol regulatory element. Proc Natl Acad Sci. 1993; 90: 11603–11607. https://doi.org/10.1073/pnas.90.24.11603 PMID: 7903453

26. Luo J, Yang H, Song B-L. Mechanisms and regulation of cholesterol homeostasis. Nat Rev Mol Cell Biol. 2020; 21: 225–245. https://doi.org/10.1038/s41580-019-0190-7 PMID: 31848472

27. Pirinen E, Gylling H, Itkonen P, Yaluri N, Heikkinen S, Pietilä M, et al. Activated polyamine catabolism leads to low cholesterol levels by enhancing bile acid synthesis. Amino Acids. 2010; 38: 549–560. https://doi.org/10.1007/s00726-009-0416-7 PMID: 19956992

28. Brown AP, Morrissey RL, Crowell JA, Levine BS. Difluoromethylornithine in combination with tamoxifen in female rats: 13-week oral toxicity study. Cancer Chemother Pharmacol. 1999; 44: 475–483. https://doi.org/10.1007/s002800051121 PMID: 10550568

29. Lu F, Liang Q, Abi-Mosleh L, Das A, Brabander JKD, Goldstein JL, et al. Identification of NPC1 as the target of U18666A, an inhibitor of lysosomal cholesterol export and Ebola infection. eLife. 2015; 4. https://doi.org/10.7554/eLife.12177 PMID: 26646182

30. Firpo MR, Mounce BC. Diverse Functions of Polyamines in Virus Infection. Biomolecules. 2020; 10: 628. https://doi.org/10.3390/biom10040628 PMID: 32325677

31. Igarashi K, Kashiwagi K. Polyamines: mysterious modulators of cellular functions. Biochem Biophys Res Commun. 2000; 271: 559–564. https://doi.org/10.1006/bbrc.2000.2601 PMID: 10814501

32. Igarashi K, Kashiwagi K. The functional role of polyamines in eukaryotic cells. Int J Biochem Cell Biol. 2019; 107: 104–115. https://doi.org/10.1016/j.biocel.2018.12.012 PMID: 30578954

33. Tauc M, Cougnon M, Carcy R, Melis N, Hauet T, Pellerin L, et al. The eukaryotic initiation factor 5A (eIF5A1), the molecule, mechanisms and recent insights into the pathophysiological roles. Cell Biosci. 2021; 11: 219. https://doi.org/10.1186/s13578-021-00733-y PMID: 34952646

34. Dever TE, Gutierrez E, Shin B-S. The hypusine-containing translation factor eIF5A. Crit Rev Biochem Mol Biol. 2014; 49: 413–425. https://doi.org/10.3109/10409238.2014.939608 PMID: 25029904

35. Rossi D, Galvão FC, Bellato HM, Boldrin PEG, Andrews BJ, Valentini SR, et al. eIF5A has a function in the cotranslational translocation of proteins into the ER. Amino Acids. 2014; 46: 645–653. https://doi.org/10.1007/s00726-013-1618-6 PMID: 24306454

36. Albulescu L, Wubbolts R, van Kuppeveld FJM, Strating JRPM. Cholesterol shuttling is important for RNA replication of coxsackievirus B3 and encephalomyocarditis virus. Cell Microbiol. 2015; 17: 1144–1156. https://doi.org/10.1111/cmi.12425 PMID: 25645595

37. Aizaki H, Morikawa K, Fukasawa M, Hara H, Inoue Y, Tani H, et al. Critical Role of Virion-Associated Cholesterol and Sphingolipid in Hepatitis C Virus Infection. J Virol. 2008; 82: 5715–5724. https://doi.org/10.1128/JVI.02530-07 PMID: 18367533

38. Bajimaya S, Frankl T, Hayashi T, Takimoto T. Cholesterol is required for stability and infectivity of influenza A and respiratory syncytial viruses. Virology. 2017; 510: 234–241. https://doi.org/10.1016/j.virol.2017.07.024 PMID: 28750327

39. Carro AC, Damonte EB. Requirement of cholesterol in the viral envelope for dengue virus infection. Virus Res. 2013; 174: 78–87. https://doi.org/10.1016/j.virusres.2013.03.005 PMID: 23517753

40. Charlton FW, Hover S, Fuller J, Hewson R, Fontana J, Barr JN, et al. Cellular cholesterol abundance regulates potassium accumulation within endosomes and is an important determinant in bunyavirus entry. J Biol Chem. 2019; 294: 7335–7347. https://doi.org/10.1074/jbc.RA119.007618 PMID: 30804209

41. Krieger SE, Kim C, Zhang L, Marjomaki V, Bergelson JM. Echovirus 1 Entry into Polarized Caco-2 Cells Depends on Dynamin, Cholesterol, and Cellular Factors Associated with Macropinocytosis. J Virol. 2013; 87: 8884–8895. https://doi.org/10.1128/JVI.03415-12 PMID: 23740983

42. Mounce BC, Poirier EZ, Passoni G, Simon-Loriere E, Cesaro T, Prot M, et al. Interferon-Induced Spermidine-Spermine Acetyltransferase and Polyamine Depletion Restrict Zika and Chikungunya Viruses. Cell Host Microbe. 2016; 20: 167–177. https://doi.org/10.1016/j.chom.2016.06.011 PMID: 27427208

43. Lu B, Liang X, Scott GK, Chang CH, Baldwin MA, Thomas T, et al. Polyamine inhibition of estrogen receptor (ER) DNA-binding and ligand-binding functions. Breast Cancer Res Treat. 1998; 48: 243–257. https://doi.org/10.1023/a:1005949319064 PMID: 9598871

44. Vijayanathan V, Thomas TJ, Nair SK, Shirahata A, Gallo MA, Thomas T. Bending of the estrogen response element by polyamines and estrogen receptors alpha and beta: a fluorescence resonance

energy transfer study. Int J Biochem Cell Biol. 2006; 38: 1191–1206. https://doi.org/10.1016/j.biocel.2005.12.015 PMID: 16767802

45. Olsen ME, Filone CM, Rozelle D, Mire CE, Agans KN, Hensley L, et al. Polyamines and Hypusination Are Required for Ebolavirus Gene Expression and Replication. mBio. 2016; 7. https://doi.org/10.1128/mBio.00882-16 PMID: 27460797

46. Cáceres CJ, Angulo J, Contreras N, Pino K, Vera-Otarola J, López-Lastra M. Targeting deoxyhypusine hydroxylase activity impairs cap-independent translation initiation driven by the 5'untranslated region of the HIV-1, HTLV-1, and MMTV mRNAs. Antiviral Res. 2016; 134: 192–206. https://doi.org/10.1016/j.antiviral.2016.09.006 PMID: 27633452

47. Hoque M, Hanauske-Abel HM, Palumbo P, Saxena D, D'Alliessi Gandolfi D, Park MH, et al. Inhibition of HIV-1 gene expression by Ciclopirox and Deferiprone, drugs that prevent hypusination of eukaryotic initiation factor 5A. Retrovirology. 2009; 6: 90. https://doi.org/10.1186/1742-4690-6-90 PMID: 19825182

48. Olsen ME, Connor JH. Hypusination of eIF5A as a Target for Antiviral Therapy. DNA Cell Biol. 2017; 36: 198–201. https://doi.org/10.1089/dna.2016.3611 PMID: 28080131

49. Dobin A, Davis CA, Schlesinger F, Drenkow J, Zaleski C, Jha S, et al. STAR: ultrafast universal RNA-seq aligner. Bioinformatics. 2013; 29: 15–21. https://doi.org/10.1093/bioinformatics/bts635 PMID: 23104886

50. Anders S, Pyl PT, Huber W. HTSeq—a Python framework to work with high-throughput sequencing data. Bioinformatics. 2015; 31: 166–169. https://doi.org/10.1093/bioinformatics/btu638 PMID: 25260700

51. Love MI, Huber W, Anders S. Moderated estimation of fold change and dispersion for RNA-seq data with DESeq2. Genome Biol. 2014; 15: 550. https://doi.org/10.1186/s13059-014-0550-8 PMID: 25516281

52. Stephens M. False discovery rates: a new deal. Biostatistics. 2017; 18: 275–294. https://doi.org/10.1093/biostatistics/kxw041 PMID: 27756721

53. Korotkevich G, Sukhov V, Budin N, Shpak B, Artyomov MN, Sergushichev A. Fast gene set enrichment analysis. 2021 Feb p. 060012. https://doi.org/10.1101/060012

54. Liberzon A, Subramanian A, Pinchback R, Thorvaldsdóttir H, Tamayo P, Mesirov JP. Molecular signatures database (MSigDB) 3.0. Bioinformatics. 2011; 27: 1739–1740. https://doi.org/10.1093/bioinformatics/btr260 PMID: 21546393